



HAL
open science

Electrochemical reduction of quinones in ethaline chosen as an example of deep eutectic solvent

Fangchen Zhen, Philippe Hapiot

► To cite this version:

Fangchen Zhen, Philippe Hapiot. Electrochemical reduction of quinones in ethaline chosen as an example of deep eutectic solvent. *Electrochemical Science Advances*, 2023, 3 (3), pp.e2100148. 10.1002/elsa.202100148 . hal-03823032

HAL Id: hal-03823032

<https://univ-rennes.hal.science/hal-03823032>

Submitted on 20 Oct 2022

HAL is a multi-disciplinary open access archive for the deposit and dissemination of scientific research documents, whether they are published or not. The documents may come from teaching and research institutions in France or abroad, or from public or private research centers.

L'archive ouverte pluridisciplinaire **HAL**, est destinée au dépôt et à la diffusion de documents scientifiques de niveau recherche, publiés ou non, émanant des établissements d'enseignement et de recherche français ou étrangers, des laboratoires publics ou privés.

Electrochemical reduction of quinones in Ethaline chosen as an example of Deep Eutectic Solvent.

*Fangchen Zhen and Philippe Hapiot**

Univ Rennes, CNRS, ISCR – UMR 6226, F-35000 Rennes, France

Abstract

The electrochemical reduction of a series of substituted benzoquinone have been examined in ethaline chosen as an example of ionic deep eutectic solvent. Experiments show the importance of hydrogen-bonding interactions between the quinone intermediates and the solvent. The effects are notably visible on the values of reduction potentials that much more positive in ethaline than in a molecular solvent like acetonitrile and the small difference between the first and second reduction potentials. The amplitude of the stabilization increases with the donor character of the substituent. Concerning the second reduction, the peak currents are considerably smaller than those of the first reduction and almost disappear at high scan rates (above 50 V s^{-1}). This behavior could be explained considering a chemical step prior to the electron transfer that becomes the limiting step (CE mechanism). As a remarkable feature, the electron transfer kinetics remain fast despite the hydrogen-bonding interactions ($k_s = 0.12 - 0.14 \text{ cm s}^{-1}$).

1. Introduction

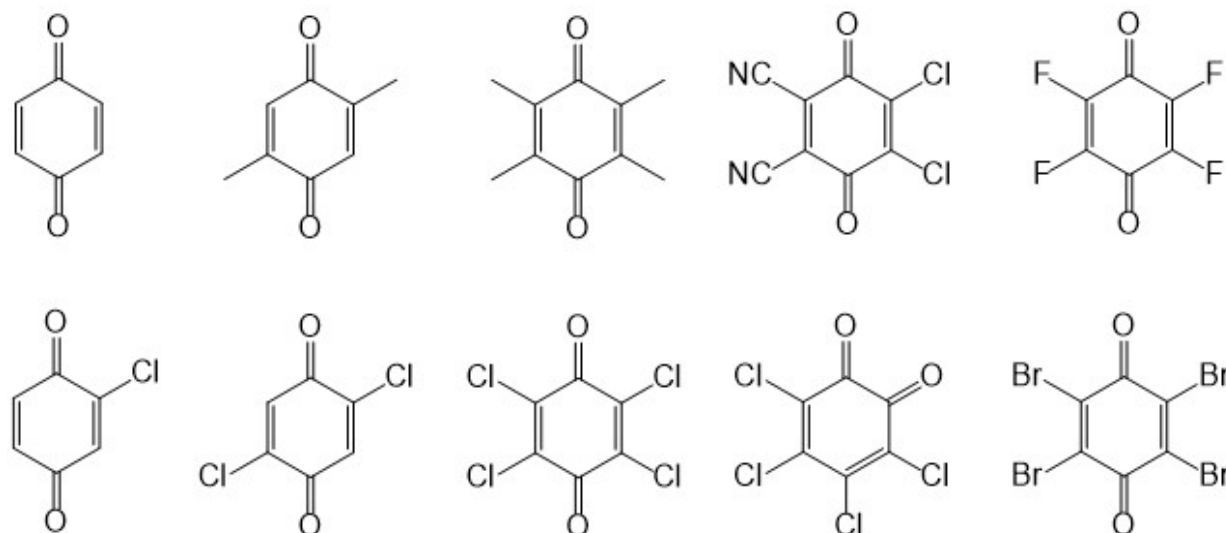
Deep Eutectic Solvents (DES) that are composed of a salt and a hydrogen bond donor have been proposed for numerous applications in electrochemistry notably as an alternative to room temperature ionic liquids (RTILs).^{1,2,3,4} As RTILs, these DES could be used in electrochemistry as electrolytic media thanks to an inherent conductivity associated to excellent solubilizing properties. To get a better description of these solvents and their interest in electrochemistry, we

have previously examined the basic redox properties of reversible monoelectronic couples (ferrocene/ferrocenium and ferrocyanide/ferricyanide) in some common DES based on choline salts.^{5,6} The electron transfer kinetic rate constants, k_s were compared with those in ionic liquids and other classical organic solvents (acetonitrile and water) and found being just a little lower than those measured in the classical solvents.^{5,6} These results contrast with observations in ionic liquids where k_s are generally largely slower (100 times lower).

In this work, we focus on redox systems where the electron transfer steps are coupled to chemical reactions. Quinones and their substituted derivatives are well adapted for such investigations because they associate the electron transfer to proton transfer and their electrochemical properties are strongly affected by hydrogen bonding^{7,8,9,10} as those existing in DES. Theoretical studies have indeed confirmed that a variety of hydrogen bonds exist between all components of the DES.¹¹ This also creates the possibility of numerous combinations between the electrochemical and chemical steps as in the proton-coupled electron transfers (PCET).¹² Although the redox behavior of quinones has been studied for many decades (see for example the introduction of reference 10 or a review in reference 13), few studies have been dedicated to their electrochemical properties in solvents like ionic DES. In relation with the present work, some investigations have concerned the reduction of quinone in ionic liquids that have been analyzed in view of the mechanisms reported in molecular solvents taking into account the strength of the hydrogen-bonding characteristics of the ionic liquids.^{14,15,16,17,18} Quinones were notably selected as model compounds for evaluating the properties of ionic liquids as electrolytes and compared with molecular solvents.¹⁸ Besides the basic studies, this also led to electrochemical applications in selected ionic liquids as the CO₂ separation from a gas mixture.¹⁷

In the present study, we have examined the reduction in ethaline of the quinones shown on Scheme 1 where different substituents are introduced on the ring. This is expected to modify the density of negative charge and basicity on the oxygen atoms and thus the stability of the electrogenerated intermediates.¹⁹





Scheme 1. Structures of the quinones and DES (Ethaline) studied in this work.

2. General Observations

Reduction of 1,4 benzoquinone.

Cyclic voltammetry recorded on a 1 mm-diameter disk glassy carbon electrode of the reduction in dry ethaline of 1,4-benzoquinone that represents the unsubstituted member of the series are presented on Figure 1. Experiments were performed in a glove box and ethaline was specially prepared to limit the presence of water that was around $2.6 \cdot 10^{-2} \text{ mol L}^{-1}$ or lower. A low scan rates ($0.05 - 1 \text{ V s}^{-1}$), a well-defined electrochemical process is visible at a potential in the range of -0.53 V . The reversibility of the process increases with the scan rate passing from an almost totally irreversible reduction at a scan rate of 0.05 V s^{-1} to a partial reversibility around 45-50% at a scan rate of 1 V s^{-1} . Another peak appears in oxidation (around 0.5 V) when the reduction peak of the benzoquinone is scanned beforehand. By comparing with an authentic sample studied in ethaline, this peak was ascribed to the oxidation of the hydroquinone indicating that the reduction of benzoquinone leads to the formation of the corresponding hydroquinone as in molecular protic solvents. As other general observation, the diffusion coefficient D is estimated around $1.8 \cdot 10^{-7} \text{ cm}^2 \text{ s}^{-1}$ that is in the range of what we have found for molecules of similar size in ethaline.^{5,6}

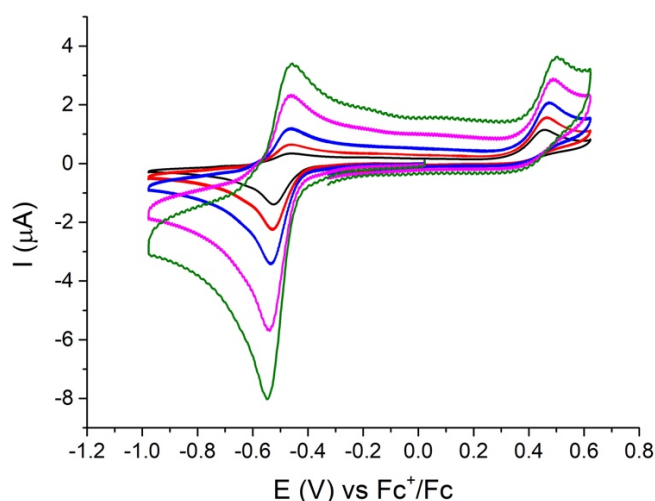
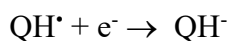
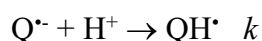
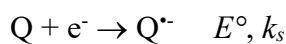


Figure 1. Cyclic voltammograms of $3.7 \cdot 10^{-3} \text{ mol L}^{-1}$ of 1,4-benzoquinone in ethaline on a 1 mm-diameter disk glassy carbon electrode at different scan rates : 0.05, 0.1, 0.2, 0.5 and 1 V s^{-1} . Conc of water : $2.6 \cdot 10^{-2} \text{ mol L}^{-1}$. Temp. = 313 K.

The reduction of quinones in presence of a low amount of proton source could be described by an ECE mechanism^{10,12} (electrochemical-chemical-electrochemical) where a radical anion forms at a first step followed by a protonation and a second reduction step leading to a global 2-electron process.^{20,21}



The observed behavior in ethaline could be analyzed with this mechanism scheme, the initially formed radical anion, $Q^{\bullet-}$ reacts with a proton sources to QH^{\bullet} then is reduced to QH^- that finally leads the corresponding hydroquinone QH_2 . Based on simulations using the KISSA 1D software of the ECE mechanism,²² we could estimate a first order rate constant k for the decay of $Q^{\bullet-}$ around $0.6\text{-}0.8 \text{ s}^{-1}$ indicating a good stability of $Q^{\bullet-}$ in this media. (See the simulated curve Figure S1 in the supporting information part). We could also examine the electron transfer kinetics by considering the peak-to-peak potential difference ΔE_p . At 0.1 V s^{-1} , a value around 60 mV is measured that is indicative of a fast electron transfer. Notice that the measurement of the electron

transfer standard rate constant, k_s , is not possible from these sole experiments and requires using higher scan rates and a special treatment of the ohmic drop. This will be developed in the following part using a special experimental setup.

Reduction of halogen-substituted quinones in ethaline.

Figures 2 and 3 show the cyclic voltammograms of the reduction of substituted halogenated benzoquinones recorded using the same glassy carbon electrode and scan rate (0.05 V s^{-1}) for an easier comparison. Two reversible reductions are visible for the tetrasubstituted compounds. These observations are similar to those reported in a molecular solvent like acetonitrile but, the potential differences between the first and second electron transfers are much smaller than those in acetonitrile (See supporting information section).⁷

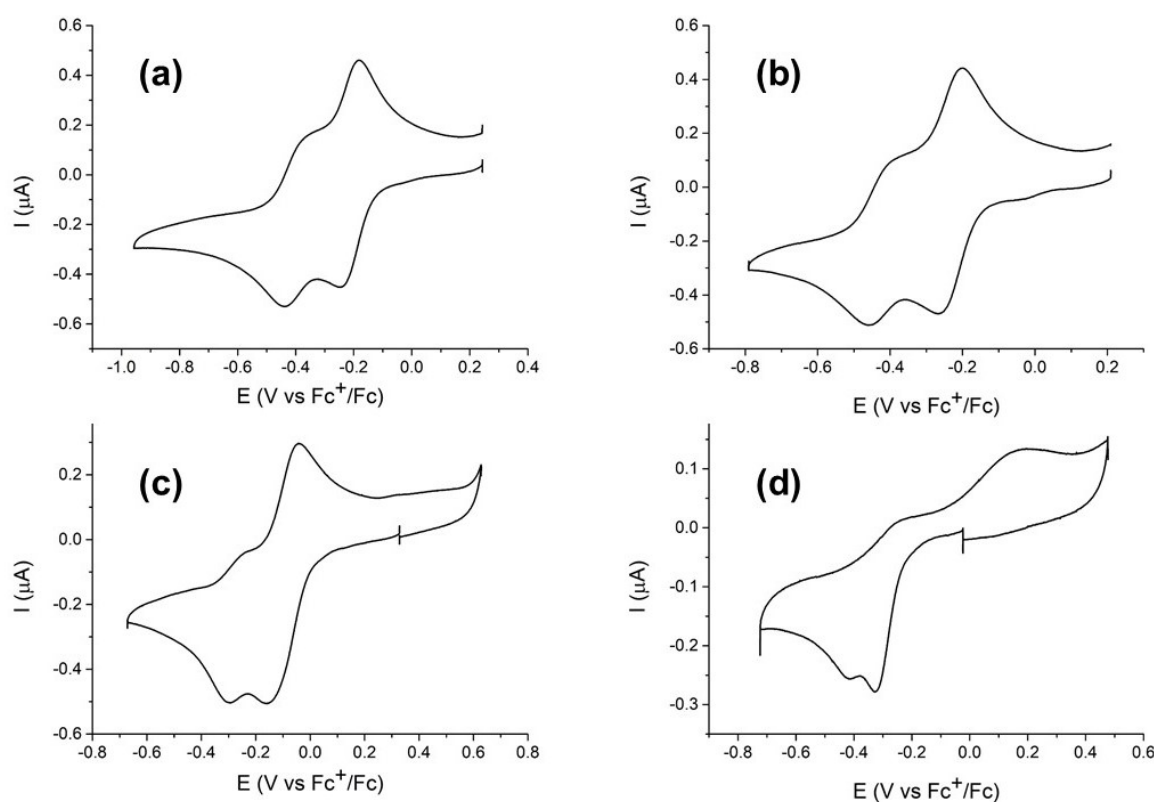


Figure 2. Cyclic voltammograms of tetra-substituted-quinone ($C^o = 2 \cdot 10^{-3} \text{ mol L}^{-1}$) in ethaline on a 1 mm-diameter disk glassy carbon electrode and at a scan rate = 0.05 V s^{-1} . (a) chloranil (tetrachloro-p-benzoquinone); (b) tetrabromo-p-benzoquinone; (c) tetrachloro-o-benzoquinone, (d) tetrafluoro-p-benzoquinone. Water concentration : $1.8 \cdot 10^{-2} \text{ mol L}^{-1}$. Temp.= 313K.

Curves recorded for the reductions of mono-chloro and dichloro quinones (See Figure 3) display similar patterns but with a more negative potential and a slightly lower reversibility indicating a higher reactivity of $Q^{\cdot-}$. As another general observation, the currents at the second reduction are considerably smaller than the current of the first reduction. Similar reports have been done in literature regarding the reduction of quinones in molecular aprotic solvent^{7,8,10} and in ionic liquids.¹⁸ Some explanations have been proposed generally based on the formation of non-electroactive species after the first reduction, but the question remains largely open. (See the discussion part below).

As seen on Figure 2d, the case of tetrafluoro benzoquinone is different. The reduction shows two irreversible processes indicating that the stabilization of the radical anion $Q^{\cdot-}$ by fluorine substituent is not sufficient to avoid its rapid decay.

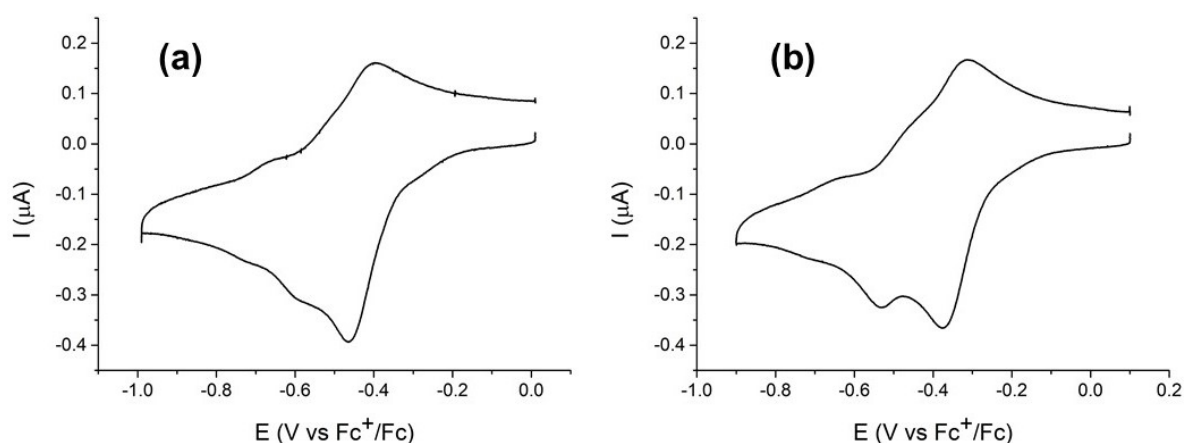


Figure 3. Cyclic voltammograms of mono and disubstituted quinones in ethaline on a 1 mm-diameter disk glassy carbon electrode at a scan rate of 0.05 V s^{-1} . (a) 2-chloro-p-benzoquinone ($C^{\circ} = 2.1 \cdot 10^{-3} \text{ mol L}^{-1}$); (b) 2,5-dichloro-p-benzoquinone ($2.0 \cdot 10^{-3} \text{ mol L}^{-1}$). Water concentration: $1.8 \cdot 10^{-2} \text{ mol L}^{-1}$. Temp. = 313 K.

Reductions of quinones with strong withdrawing or donor substituents. To complete the study, we have examined the electrochemistry of other quinones in ethaline bearing strong withdrawing substituent or donor substituents. Figure 4 shows the cyclic voltammetry of the reduction of 2,3-dichloro-5,6-dicyano-p-benzoquinone in ethaline at low scan rate. Analysis of the peak current and taking the first reduction of chloranil as a $1e^{-}$ standard shows that the reduction is mono-electronic. It corresponds to the reversible formation of the radical anion in ethaline as expected from a good stabilization of the electrogenerated $Q^{\cdot-}$ by the two cyano groups. A more surprising

observation is the quasi-absence of a second reduction process. In fact, a second process is actually visible around -0.5 V but its peak current is much smaller (it is only 25 % of the first reduction) similar to the above observations that second peak currents are considerably smaller in ethaline. Another broad intermediate process is also visible between the two peaks (in the 0.1 V potential zone) that may be due to the carbon electrode as proposed previously.¹⁰

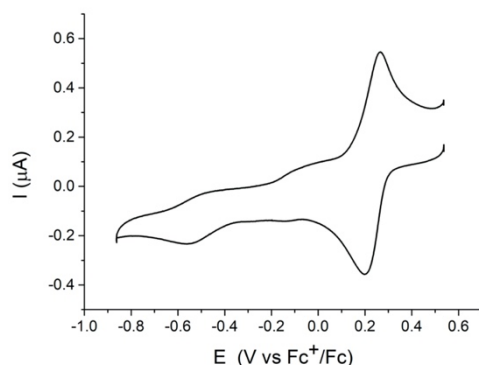


Figure 4. Cyclic voltammogram on 1 mm diameter glassy carbon electrode of $2.1 \cdot 10^{-3} \text{ L}^{-1}$ 2,3-dichloro-5,6-dicyano-p-benzoquinone on a 1 mm-diameter disk glassy carbon electrode in ethaline at 313 K at scan rate of 0.05 V s^{-1} . Water concentration : $1.8 \cdot 10^{-2} \text{ mol L}^{-1}$.

As seen on Figure 5, reductions of dimethyl-substituted and tetramethyl-quinone (duroquinone) also display sort of reversible cyclic voltammograms. However, the analysis of the peak current intensity shows a global stoichiometry of $2e^-$ taking the reduction of chloranil as a $1e^-$ standard. The reduction peak currents characterized by their half peak width ($E_p - E_{p/2}$) are much thinner with $E_p - E_{p/2} \approx 38 \text{ mV}$ (corresponding to the simultaneous transfer of 2-electron process, theory 28 mV) than peak currents of the other quinones with $E_p - E_{p/2} \approx 63\text{-}65 \text{ mV}$.^{23,24} Contrarily to the reduction of benzoquinone, the reversibility does not increase with the scan rate and the return peaks takes a more plateau shape when the scan rate is increased with the appearance of new peaks (See Figure S2 in the supplementary material part or the reference²⁵). Such behavior could be explained by the same general ECE mechanism when the chemical steps are fast and partially at the equilibrium. In the framework of the $(ECE)_{\text{rev}}$ mechanism, increasing the scan rate makes the equilibrium less reversible and thus the global reversibility of the process decreases. This leads to a more irreversible process and appearance of new peaks due to the direct reoxidation of intermediates in the ECE mechanism.²¹

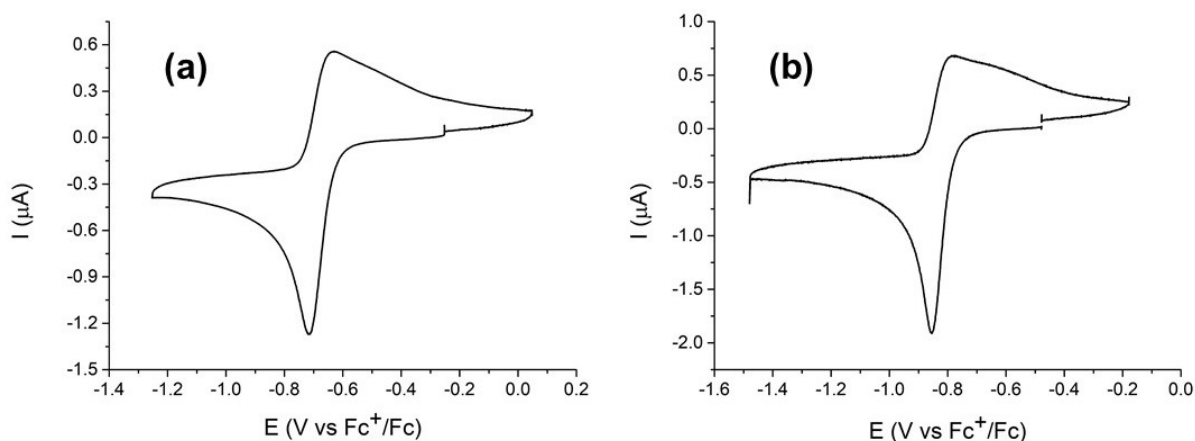


Figure 5. Cyclic voltammetry of the reduction of quinones with donor groups in ethaline on a 1 mm-diameter disk glassy carbon electrode. Solution of (a) $2.3 \cdot 10^{-3} \text{ mol L}^{-1}$ dimethylquinone and (b) $2.1 \cdot 10^{-3} \text{ mol L}^{-1}$ duroquinone in ethaline. Temp: 313 K. Scan rate 0.05 V s^{-1} Water concentration: $1.8 \cdot 10^{-2} \text{ mol L}^{-1}$.

3. Results and Discussions.

Diffusion coefficients of quinones in Ethaline.

The characteristics of the quinones reductions in ethaline are reported in Table 1. The derived diffusion coefficients, D , were calculated from the first peak current I_p considering the prevailing kinetics control.^{20,21,23} For the reversible 1-electron system, they were derived using the relation for a reversible monoelectronic process: $I_p = 0.446 FSC\sqrt{D} \sqrt{\frac{Fv}{RT}}$ where F is the Faraday constant, S the electrode surface area, C the initial concentration of the redox couple, R the gas constant, v the scan rate and T the absolute temperature. For the fully bielectronic couple (2,5-dimethyl-p-benzoquinone and duroquinone), to take into account the thinner peak of an $(ECE)_{\text{rev}}$ mechanism we considered the equation for the simultaneous transfer of 2 electrons, $n=2$ and $I_p = 0.446 nFSC\sqrt{D} \sqrt{\frac{nFv}{RT}}$.^{20,21} Finally, the relation for the $EC_{\text{irr}}E$ mechanism, $I_p = 0.496 nFSC\sqrt{D} \sqrt{\frac{Fv}{RT}}$ was used for the analysis of the benzoquinone voltammogram ($n=2$).^{20,21} The diffusion coefficients in ethaline of the different quinones are all in the $1.5 - 2 \cdot 10^{-7} \text{ cm}^2 \text{ s}^{-1}$ range. They are two orders smaller than in those in a molecular solvent like acetonitrile reflecting the higher viscosities of ethaline.^{5,6} In that sense, the mass transport of quinones in ethaline does not reveal a special behavior compared to other redox molecules like ferrocene.

Table 1. Electrochemical parameters for the reduction of quinones in Ethaline at 313K.

Quinone	E_p^1/V	$\Delta E^1/mV$	E_p^2/V	$D/cm^2 s^{-1}$	n
2,3-Dichloro-5,6-dicyano-p-benzoquinone	0.20	60	-0.56	1.7×10^{-7}	1
Tetrachloro-o-benzoquinone	-0.16	83	-0.29	2.2×10^{-7}	1
2,3,5,6-Tetrachloro-p-benzoquinone (Chloranil)	-0.24	58	-0.44	2.0×10^{-7}	1
2,3,5,6-Tetrabromo-p-benzoquinone	-0.26	62	-0.46	1.6×10^{-7}	1
2,3,5,6-Tetrafluoro-p-benzoquinone	-0.33	-	-	1.5×10^{-7}	1
2-chloro-p-benzoquinone	-0.46	65	-	2.0×10^{-7}	1
2,5-Dichloro-p-benzoquinone	-0.38	64	-	1.5×10^{-7}	1
p-Benzoquinone	-0.53	62	-	1.8×10^{-7}	2
2,5-Dimethyl-p-benzoquinone	-0.72	-	-	1.6×10^{-7}	2
2,3,5,6-Tetramethyl-p-benzoquinone (Duroquinone)	-0.85	-	-	2.2×10^{-7}	2

E_p^1 : Peak potentials of the first reduction E_p^2 : Peak potentials of the second reduction peak. ΔE^1 : Peak to peak difference of the first reduction measured at $0.05 V s^{-1}$ from reversible or partially reversible voltammograms. All potentials are measured versus the Fc^+/Fc couple in ethaline.

Reduction potentials in ethaline. Comparison with data in acetonitrile.

We could compare the redox potentials of Table 1 in ethaline with those measured in acetonitrile containing $0.1 mol L^{-1} NBu_4PF_6$ as supporting electrolyte. Reduction potentials reflect the interactions of the quinone and of its radical anion with the electrolyte solvent.^{7,8,9,10} In an ionic liquid or in a DES like ethaline, the supporting electrolyte that is also the solvent, could participate in ion-pairing or H-bonding interactions with the reduced quinone forms, whereas the polarity of the solvent also affects the solvation energies.^{15,18} Rigorously, such correlation would require the measurement of the thermodynamic data, *i.e.* the standard potentials E° that could only be derived from a reversible voltammogram.^{20,21} If the reduction of quinones in acetonitrile presents reversible processes, only few of the studied quinone reductions were found to be totally reversible in ethaline. Our comparison on Figure 6 was thus based on the peak potential variations E_p , but covers a large change in the reduction power that is much higher than 1 V. Even if different kinetics controls could prevail in the ECE mechanism that may introduce deviations between E_p

We could also consider the potential difference between the first and the second reduction. In a molecular solvent like acetonitrile containing a quaternary ammonium salt as supporting electrolyte, the two reductions of a quinone derivative are generally separated by about 0.7 V (See supplementary Section for the studied quinones). As seen in Table 1 in ethaline, with the exception of 2,3-dichloro-5,6-dicyano-p-benzoquinone, the potential differences between the first and the second transfers are only 0.2-0.3 V. This falls in line with a higher stabilization of the charged species by the solvent and confirms the occurrence of strong H-bonding interactions.⁷

Electron transfer kinetics of the quinone reduction in ethaline.

Electron transfer rate constant k_s is another important parameter besides the reduction potentials for detecting the presence of a specific solvation. In the framework of the Marcus theory, the standard rate constant corrected by the effect of the double layer for an adiabatic electron transfer is given by:^{27,28}

$$k_s = \frac{K_p}{\tau_L} \left(\frac{\Delta G_{Os}^\#}{4\pi RT} \right)^{1/2} \exp \left[- \left(\frac{\Delta G_{Os}^\# + \Delta G_{is}^\#}{RT} \right) \right]$$

where K_p is the equilibrium constant for a precursor complex and τ_L is the longitudinal relaxation time that is the relaxation time of the solvent normalized by the ratio of the static ϵ_s and high frequency ϵ_{op} relative permittivities, $\Delta G_{Os}^\#$, $\Delta G_{is}^\#$ are the standard Gibbs activation energy of the outer sphere and inner sphere contributions. $\Delta G_{Os}^\#$ reflects the change of solvation between the neutral quinone and the produced radical anion. In this part, we focus on the electrochemical properties of the tetra-bromo and tetra-chloro quinones that present the simplest patterns. Such investigations in a DES are quite challenging as they require using high scan rates.⁶ The main difficulties arise both from the higher resistivity and the lower viscosity of a DES like ethaline. Higher resistivity results in higher residual ohmic drop that make unusable the curves recorded at high scan rates for a quantitative analysis. About higher viscosity, it also means lower diffusion coefficients. Because D are smaller, the measurement of the standard rate for a given k_s constant requires using much higher scan rates in ethaline as the determining kinetics parameter Λ is

$$\Lambda = \frac{k_s}{\sqrt{D}} \sqrt{\frac{RT}{aFv}}$$
 Λ should be lower than 1 for allowing the determination (α is the transfer coefficient). Experiments in ethaline require a special setup in which the ohmic drop could be effectively compensated.^{29,30} Fast scan rate voltammograms using a 1 mm-diameter disk glassy carbon electrode are shown on Figures 7 and 8. Use of the positive feedback compensation explain the extra-noise that is visible on these curves.

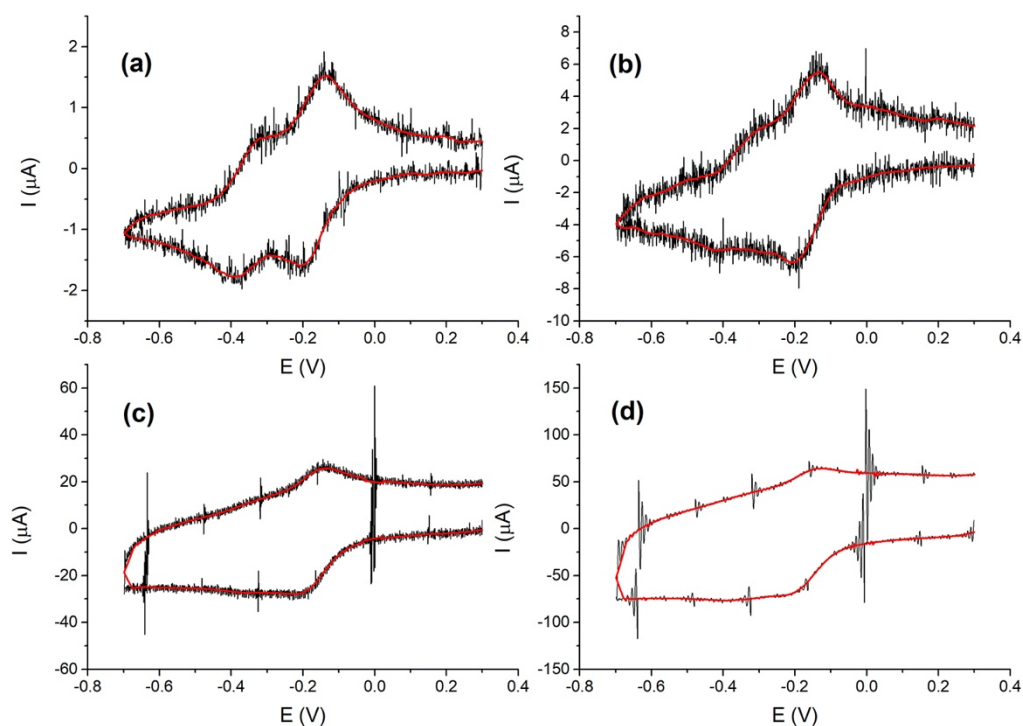


Figure 7. High scan rate cyclic Voltammetry of $2 \cdot 10^{-3} \text{ mol L}^{-1}$ chloranil solution in ethaline on a 1 mm-diameter disk glassy carbon electrode. Scan rates (a) 0.5 (b) 5 (c) 50 (d) 200 V s^{-1} . Temp. = 303 K. Concentration of water: $2.8 \cdot 10^{-2} \text{ mol L}^{-1}$.

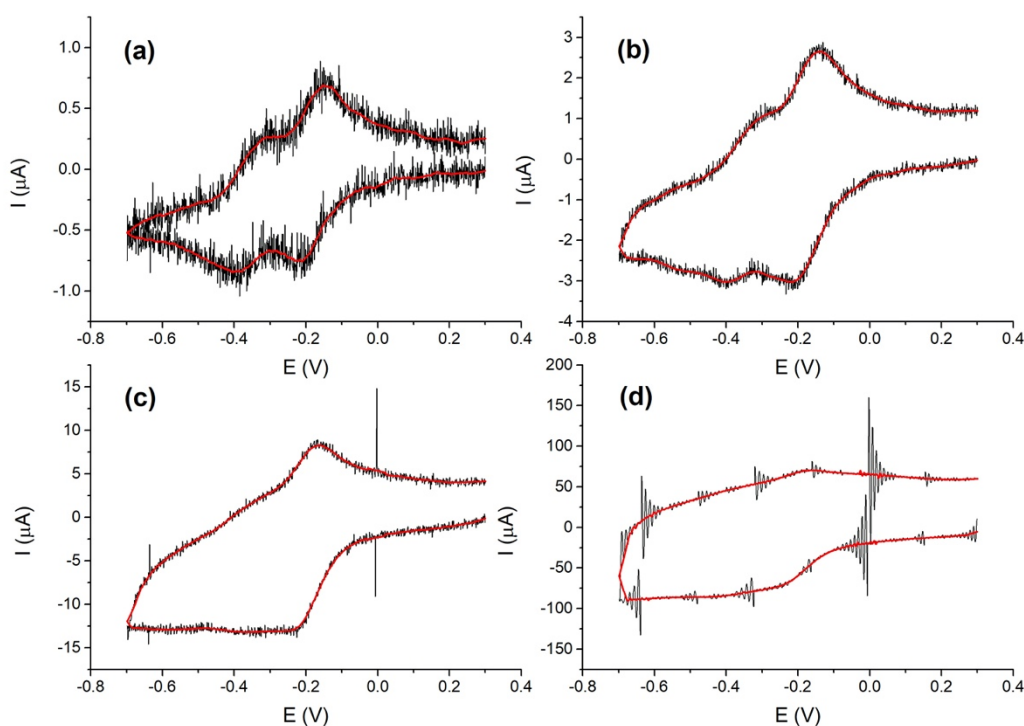


Figure 8. High scan rate cyclic voltammetry of $2.0 \cdot 10^{-3} \text{ mol L}^{-1}$ tetrabromo-p-benzoquinone solution in ethaline on a 1 mm-diameter disk glassy carbon electrode. Scan rates : (a) 0.2 (b) 2 (c) 20 (d) 200 V s^{-1} Temp. = 303 K. Concentration of water: $2.8 \cdot 10^{-2} \text{ mol L}^{-1}$.

The value of the standard rate charge transfer constant k_s were derived from the variation of the peak-to-peak potential with the scan rate following previously described procedures.^{5,20,21} Figure 9 shows the experimental ΔE_p versus log of the scan rate for the first reduction as the fit with the theoretical variations. The adjustment between experimental and calculated variations provides a unique determination the experimental parameter $k_s/D^{1/2}$. For both quinones, ΔE_p does not considerably vary for most of the low scan rates range and only increases for the highest scan rates. This is indicative of a high value of parameter $k_s/D^{1/2}$ that could be measured as 230 and 295 s^{-1} for the first reduction of chloranil and tetra-bromo-p-benzoquinone respectively. Taking into account the D values, we derived k_s values of 0.12 cm s^{-1} for the reduction of chloranil and 0.14 cm s^{-1} for the reduction of tetra-bromoquinone. These values are higher than the charge transfer rates for a couple like ferri/ferrocyanide in the same conditions ($2 \cdot 10^{-2} \text{ cm s}^{-1}$) but remain slower than the transfer rate of a fast system like the ferrocene/ferrocenium couple,⁶ a ranking that is similar to what is expected in a classical molecular solvent like acetonitrile.

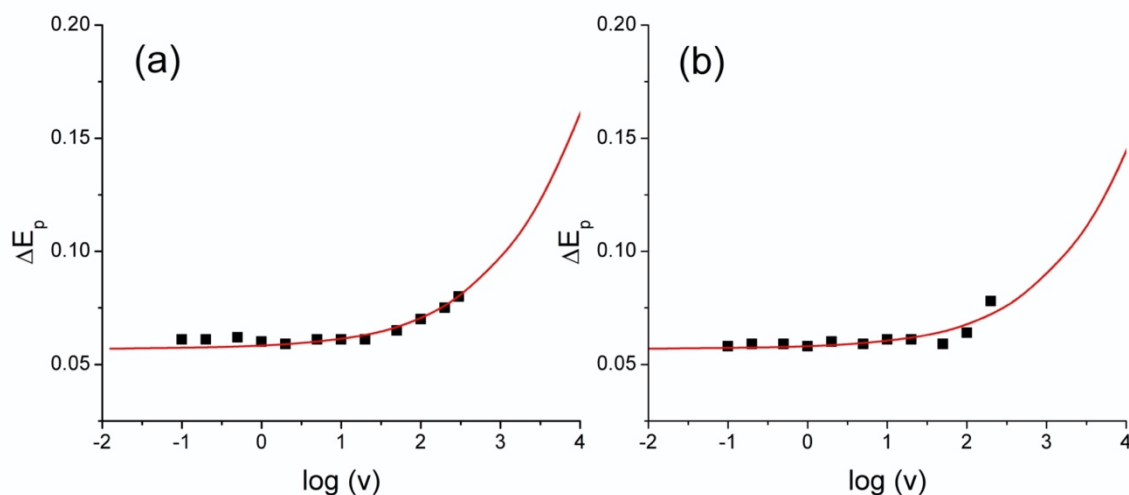


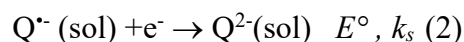
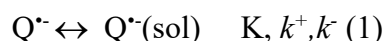
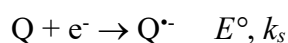
Figure 9. Variation of the peak potential ΔE_p with the scan rate. (a) Reduction of chloranil in Ethaline. (b) Reduction of tetrabromo-p-benzoquinone in ethaline. Temp.: 303 K. Working electrode is a 1 mm-diameter disk glassy carbon electrode. Lines are the theoretical behavior assuming a Butler-Volmer Law and a transfer coefficient α equal to 0.5.⁶

Second reduction of quinones in ethaline.

As noticed above, for all the studied quinones, the peak current of the second reduction in ethaline is considerably smaller than the one of the first reduction, the difference depending on the structure of the quinone and substituents. Similar observations were reported in numerous publications (see for examples references 7,8,10 and the references therein) for the reduction of substituted quinones in molecular solvents and in imidazolium based ionic liquids.¹⁸ A simple explanation could be a difference of diffusion coefficients between the radical anion $Q^{\cdot-}$ and the neutral quinone Q resulting of a second smaller peak. Such explanation does not sound for a molecular solvent or in ethaline where the diffusion coefficients present negligible variations with the charge of the molecule.^{5,6} Notice that because of the occurrence of homogeneous electron transfer reactions and the ensuing coupling of diffusional pathways, this will also result in a loss of reversibility of the voltammogram,³¹ which is not visible in our results. Instead, different explanations considering some forms of dimerization of $Q^{\cdot-}$ were proposed in the literature to explain the voltammetry. Among the possible mechanisms, the reaction between the neutral quinone Q and the dianion Q^{2-} yielding an electro inactive dimeric product $[Q_2]^{2-}$ was proposed for explaining the lower currents.^{7,8} These assumptions were then latter discussed. Some inconsistencies with a proposed dimerization mechanism when changing the concentration

of quinone were spotted and a different mechanism involving the association of $Q^{\cdot-}$ with the OH present on the surface of a glassy carbon electrode was proposed.¹⁰ To bring some additional highlights on this puzzling phenomenon, we could focus on the evolution of the second process on the voltammograms of Figures 6 and 7 (reductions of chloranil and tetrabromobenzoquinone in ethaline). At low scan rate (Figure 2a,b), the second peak is reversible and smaller than the first process as reported before. When the scan rate is increased, the second peak becomes broader and more unsymmetric, the return peak current being larger than the forward peak current. For the highest scan rate, the second peak becomes almost not visible. This observation appears incompatible with the hypothesis of the formation of a non-electroactive species (as a dimer) in a competitive manner as the reverse effect with the scan rate is expected.⁸ On the contrary, the behavior observed in ethaline is understandable in the framework of a CE mechanism where a chemical step precedes the second electron transfer. Based on the above observations, it is likely that such chemical step be a specific interaction with the media notably by hydrogen-bonding or with a low amount of proton donor in the literature leading to the more reducible $Q^{\cdot-}(\text{sol})$.^{7,9} If it is difficult to clearly identify the nature of 'sol', we have not observed considerable changes of the voltammograms when the amount of water was doubled.

The CE mechanism is characterized by a large a variety of possible voltammograms shapes depending on competition between diffusion and the homogeneous preceding reaction that is characterized by its equilibrium constant K , and a kinetics parameter $\lambda = \frac{RT}{F} \frac{(k_+ + k_-)}{v}$ with k_+ and k_- being the forward and return kinetics rate constants of the preceding chemical step:²¹



We performed simulations of the voltammograms²² assuming this mechanism (See Figure 10, notice that background currents are not introduced in the simulated curves). These simulations support the hypothesis of a CE mechanism by reproducing the general trend with a kinetics parameter $K(k_+ + k_-)^{1/2}$ in the range of $30 \text{ s}^{-1/2}$.

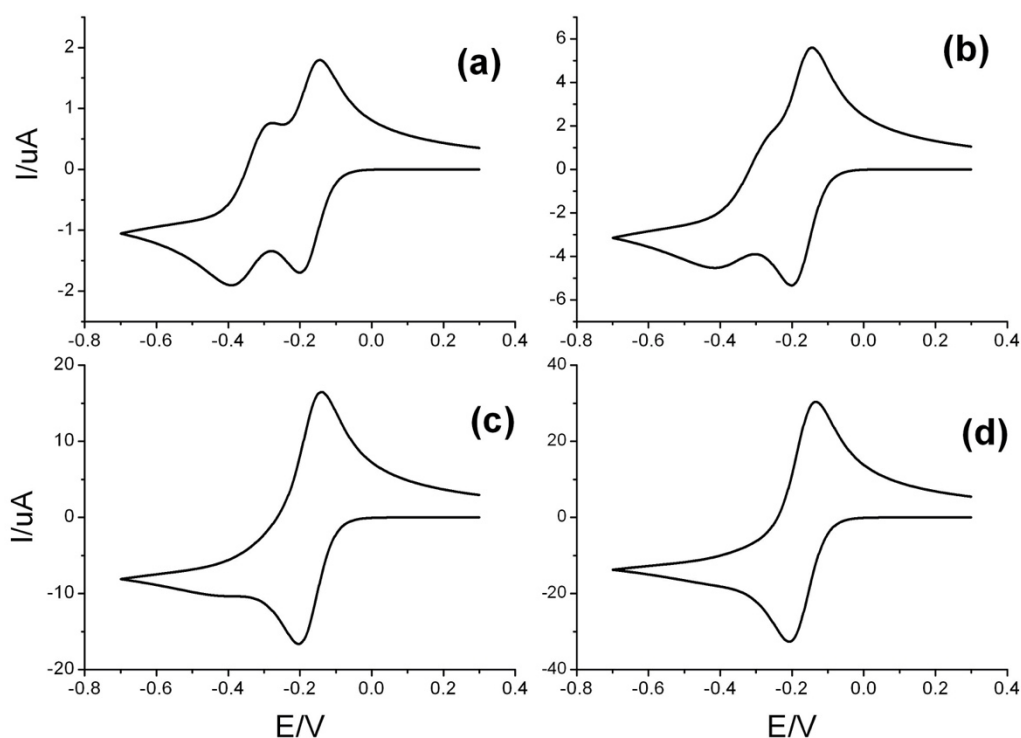


Figure 10. High scan rates cyclic Voltammometry of the reduction of chloranil in ethaline. Simulation of the experiments of Figure 7 using KISSA-1D software. Scan rate : 0.5 (b) 5 (c) 50 (d) 200 (See text for details and supplementary section for parameters used in the simulation).

4. Conclusion

The redox behavior of quinone in ethaline that is strongly dependent of the quinone nature, display many similarities with what is observed in a solvent like acetonitrile but with some notable differences as lower reduction potentials or small potential differences between the first and the second charge transfer. The reduction potentials vary in a similar manner with the substituent in acetonitrile and in ethaline but the amplitude of the variation is lower in ethaline (slope =0.71). These observations reflect the effect of H-bonding in ethaline resulting in the stabilization of the electrogenerated quinone intermediates. As an important feature for applications, the first electron transfer kinetics remain fast in ethaline despite the strong stabilization of the quinone intermediate. The second electron transfer shows also the interactions with the DES resulting in a CE mechanism that makes the second reduction much easier but with some kinetics limitations.

Experimental section

Chemicals and materials. All quinones were commercially available from Sigma-Aldrich and used as received without further purification unless specified. p-Benzoquinone was purified via reduced pressure sublimation using a cold finger sublimation apparatus before experiments. 2,3-Dichloro-5,6-dicyano-p-benzoquinone (DDQ) was recrystallized from chloroform before use. Ethaline was prepared by mixing the dried choline chloride (ChCl) and anhydrous ethylene glycol (EG) (ChCl:EG mole ratio 1:2) into a round flask in an argon-filled glovebox and then heated at 333.15 K until a homogeneous liquid was formed. Choline chloride was previously recrystallized from anhydrous ethanol and then dried in a Schlenk line under high vacuum for 90 hours to remove the water.

Electrochemical Measurements. Cyclic voltammetry experiments were done using a conventional three electrode cell, with glassy carbon working electrode (1 mm-diameter disk sealed in a glass tube), platinum grid counter electrode, and Pt/polypyrrole quasi-reference electrode using a SP-50 potentiostat from Biologic Instrument. The Pt/polypyrrole quasi-reference electrode was made according an adaptation of the published procedure³². In a solution containing 0.01 mol L⁻¹ pyrrole and 0.1 mol L⁻¹ NBu₄PF₆ in acetonitrile, PPy film is electropolymerized onto Pt wire with a platinum grid as counter electrode and saturated calomel electrode (SCE) as reference electrode in the condition of sweeping the potential at 0.1 V/s over the potential range -0.6-1.2 V for 50 cycles and stop at 0.4 V.

Quinone in ethaline solutions and cyclic voltammetry at low scan rate were made in an argon-filled glovebox, with O₂ and H₂O both below 0.5 ppm. The Pt/PPy reference electrode was immersed no less than 15 min in the solution before measurements at 313±2 K (40 degree centigrade). Ferrocene (Fc) was directly added to the solution at the end of the experiments and used as a calibrating redox couple to provide an absolute potential reference. All potentials in the text are reported versus the half-wave potential of Fc⁺/Fc couple. The half-wave potential of Fc⁺/Fc couple versus a SCE electrode measured in ethaline was found to be 0.335 V/SCE. value Based on repetitive measurements, errors on potential values are estimated as ± 10 mV. The water

amounts were measured using a Karl Fisher Coulometer (831KF Coulometer – Metrohm and using Hydranal® Coulomat E solution from Fluka) before each experiment and are in the range of 330~350 ppm ($1.8\text{-}1.9 \times 10^{-2} \text{ mol L}^{-1}$).

For fast scan rate cyclic voltammetry in ethaline (Figures 7 and 8), cyclic voltammetry experiments were done outside the glovebox at 303K and using a home-made potentiostat equipped with ohmic drop compensation.⁶ Ethaline was injected into a well-sealed cell in glovebox and then taken outside for the experiments. For typical experiments, water amount measured in the cell at the beginning of the experiment was 500 ppm, $2.8 \times 10^{-2} \text{ mol L}^{-1}$ of water.

Quinone reductions in acetonitrile (+ $0.1 \text{ mol L}^{-1} \text{ NBu}_4\text{PF}_6$) were studied outside the glovebox at room temperature (293 K) using the same electrodes (excepting the saturated calomel electrode (SCE) as reference electrode) using an Autolab PGSTAT 302N (Metrohm). The water amount measured in acetonitrile, but before adding the supporting electrolyte, was around 500 ppm, $2.8 \times 10^{-2} \text{ mol L}^{-1}$.

All calculation of cyclic voltammetry were done using the Kissa 1D package developed by C. Amatore and I. Svir using the default parameters.²²

Acknowledgements

The authors sincerely thank Corinne Lagrost and Pacquin (ISCR, Rennes) for their helpful discussions concerning the properties and preparations of ethaline. C. Amatore and I. Svir (CNRS, ENS Paris) are warmly thanked for making us available a preliminary version of the KISSA 1D package. China Scholarship council (CSC) of the People's Republic of China is thanked for a grant to FZ.

Conflict of Interest

The authors declare no conflict of interest.

References

1. A. P. Abbott, G. Capper, D. L. Davies, H. L. Munro, R. K. Rasheed, V. Tambyrajah, *Chem. Commun.* **2001**, 2010-2011.
2. A.P. Abbott, D. Boothby, G. Capper, D.L. Davies, R.K. Rasheed, *J. Am. Chem. Soc.* **2004**, *126*, 9142-9147.
3. E. L. Smith, A. P. Abbott, K. S. Ryder, *Chem. Rev.* **2014**, *114*, 11060-11082.
4. M. A. R. Martins, S. P. Pinho, J. A. P. Coutinho, *J. Sol. Chem.* **2018**, <https://doi.org/10.1007/s10953-018-0793-1>.
5. S. Fryars, E. Limanton, F. Gauffre, L. Paquin, Lagrost, P. Hapiot, *J. Electroanal. Chem.* **2018**, *819*, 214-219.
6. F. Zhen, L. Percevault, L. Paquin, E. Limanton, C. Lagrost, P. Hapiot, *J. Phys. Chem. B* **2020**, *124*, 1025-1032.
7. N. Gupta, H. Linschitz, *J. Am. Chem. Soc.* **1997**, *119*, 6384-6391.
8. M. W. Lehmann, D. H. Evans, *J. Electroanal. Chem.* **2001**, *500*, 12–20.
9. R. R. S. Shi, M. E. Tessensohn, S. J. L. Lauw, N. A. B. Y. Foo, R. D. Webster, *Chem. Commun.* **2019**, *55*, 2277.
10. P.A. Staley, C. M. Newell, D.P. Pullman, D. K. Smith, *Anal. Chem.* **2014**, *86*, 10917-10924.
11. V. Alizadeh, F. Malberg, A. A. H. Pádua, B. Kirchner, *J. Phys. Chem. B* **2020**, *124*, 7433-7443.
12. C. Costentin, M. Robert, J.-M. Savéant. *Acc. Chem. Res.* **2010**, *43*, 7, 1019-1029.
13. R. S. Kim and T. D. Chung, *Bull. Korean Chem. Soc.* **2014**, *35*, 3143-3155.
14. M. T. Carter, R. A. Osteryoung, *J. Electrochem. Soc.* **1992**, *139*, 1795-1802.
15. Y. J. Wang, E. I. Rogers, S. R. Belding, R. G. Compton, *J. Electroanal. Chem.* **2010**, *648*, 134-142.
16. S. Ernst, L. Aldous, R. G. Compton, *Chem. Phys. Lett.* **2011**, *511*, 461-465.
17. B. Gurkan, F. Simeon, T. Alan Hatton, *ACS Sustainable Chem. Eng.* **2015**, *3*, 1394-1405
18. V. A. Nikitina, R. R. Nazmutdinov, G. A. Tsirlina, *J. Phys. Chem. B* **2011**, *115*, 668-677.
19. M. T. Huynd, C. W. Anson, A. C. Cavell, S. S. Stahl, S. Hammes-Schiffer, *J. Am. Chem. Soc.* **2016**, *138*, 15903-15910.
20. A. J. Bard, L. R. Faulkner, *Electrochemical Methods Fundamentals and Applications*, 2nd ed.; John Wiley and Sons: New York, 2000.
21. J. -M. Savéant, *Elements of Molecular and Biomolecular Electrochemistry: An Electrochemical Approach to Electron Transfer Chemistry*; John Wiley & Sons, Inc.: Hoboken, 2006.

-
22. O.V Klymenko, A. Oleinick, I. Svir, C. A. Amatore, KISSA - *Software for Simulation of Electrochemical Reaction Mechanisms of Any Complexity*. <https://www.kissagroup.com/> (accessed August 19, 2021).
23. J. -M. Savéant, C. P. Andrieux, L. Nadjo, *J. Electroanal. Chem. Interfacial Electrochem.* **1973**, 41, 137-1410.
24. P. Hapiot, L. D. Kispert, V. V. Konovalov, J. -M. Savéant, *J. Am. Chem. Soc.* **2001**, 123, 6669-6677.
25. S. J. Cobb, Z. J. Ayres, M. E. Newton, J. V. Macpherson, *J. Am. Chem. Soc.* **2019**, 141, 1035-1044.
26. M. E. Tessensohn, H. Hirao, R. D. Webster, *J. Phys. Chem. C* **2013**, 117, 1081-1090.
27. J. M. Weaver, *Chem. Rev.* **1992**, 92, 463-480.
28. R.W. Fawcett, A. Gaál, D. Misicak, *J. Electroanal. Chem.* **2011**, 660, 230-233.
29. D. Garreau, J. -M. Savéant, *J. Electroanal. Chem.* **1972**, 35, 309-331.
30. D. Garreau, P. Hapiot, J. -M. Savéant, *J. Electroanal. Chem.* **1989**, 272, 1-16.
31. C. P. Andrieux, P. Hapiot, J. -M. Savéant, *J. Electroanal. Chem.* **1985**, 186, 237-246.
32. J. Ghilane, P. Hapiot, A. J. Bard, *Anal. Chem.* **2006**, 78, 19, 6868-6872.